Early rotation and late folding in the Pennsylvania salient (U.S. Appalachians): Evidence from calcite-twinning analysis of Paleozoic carbonates

Philip F. Ong
Ben A. van der Pluijm[†]
Rob Van der Voo
Department of Geological Sciences, University of Michigan, Ann Arbor, Michigan 48109-1005, USA

ABSTRACT

Calcite-twinning analysis of Paleozoic limestones from 42 sites reveals that the change in regional strike along the frontal edge of the Pennsylvania salient is accompanied by an equal-magnitude rotation of paleostress directions of up to 60 degrees. The rotations, recorded at 22 reliable sites, show no discernible difference between sites with rocks of Cambrian-Ordovician and Silurian-Devonian age. Evidence for similarly fanned orientations is not present in foreland sites. Scatter in the data is attributed to grain-scale rotations and compaction overprinting, as demonstrated in prior studies, and it was reduced by data-cleaning methods as well as by the use of contouring and data-averaging methods. Comparisons of paleostress directions within the belt reveal only minor rotations in the southwest region of the salient, and the bulk of rotation is accommodated by the northern limb. We hypothesize that these rotations resulted from convergence in the thrust wedge against a northerly bounding, rigid basement block around Pennsylvanian times. This created a structural anisotropy in the evolving belt that guided the post-rotational formation of folds in Early Permian times and produced the current pattern of the salient. This model of decoupled thrusting/rotation and folding explains a variety of previously conflicting observations in the area while offering a kinematically consistent scenario that may also apply to other curved orogenic belts.

Keywords: orocline, Appalachians, structure, fold-and-thrust belt, calcite.

INTRODUCTION

A feature of many, if not most, fold-and-thrust belts around the world is the presence of curved segments, with a degree of curvature that may range from tens of degrees to as much as 180°. Orogenic curvature had already been noted a century ago (Hobbs, 1914) and in the mid-1950s, Carey introduced the term "orocline" to describe this common geometry (Carey, 1955). Originally, orocline was used to describe a straight belt that later became curved (secondary curvature), but the term is used today to describe both originally curved segments (primary curvature) as well as secondary curvature of belts (Eldredge et al., 1985; Marshak, 1988; Hindle and Burkhard, 1999). Modern interpretations for curved belts range from primary curvature to progressive rotational displacements to secondary curvature, or combinations, based on kinematic, paleomagnetic, and modeling studies (e.g., Kollmeier et al., 2000; Weil et al., 2000; Spraggins and Dunne, 2002; Marshak, 2004; Sussman et al., 2004; Weil and Sussman, 2004).

The Pennsylvania salient, one of the more striking features of the Appalachian Mountain belt in map view, accommodates a change in orientation of structural features from a south-southwesterly direction in the central Appalachians to an easterly direction farther north near the New York–Pennsylvania border (Fig. 1). The evolution of the Pennsylvania salient remains a topic of active discussion (e.g., Wise, 2004), in large part due to seemingly conflicting kinematic and paleomagnetic data on the curvature of the belt. Paleomagnetic results indicate a prefolding rotation of 20–30° between inner segments of the salient limbs (Kent, 1988; Stamatakos and Hirt, 1994; Stamatakos et al., 1996). Kinematic data show a consistent, parallel early shortening direction that diverges clockwise in the northern salient limb and counterclockwise in the southern salient limb over time (Nickelsen, 1979; Geiser and Engelder, 1983; Gray and

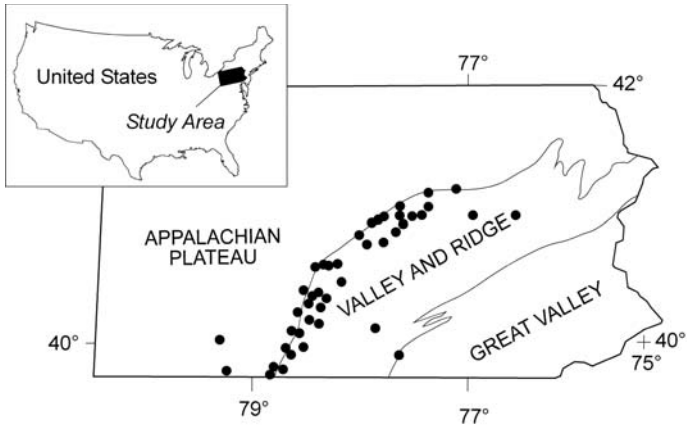

Figure 1. Generalized map of study area, where the Pennsylvania salient follows the outline of the Valley and Ridge province, with schematic boundaries. Dots mark sampling sites for this study.

[†]Corresponding author e-mail: vdpluijm@umich.edu.

GSA Bulletin; July/August 2007; v. 119; no. 7/8; p. 796–804; doi: 10.1130/B26013.1; 8 figures; 2 tables.

Mitra, 1993; Zhao and Jacobi, 1997; Younes and Engelder, 1999), and this differs with the pure-bending model typically associated with oroclinal evolution. These conflicting paleomagnetic and kinematic scenarios have prompted new hypotheses (Gray and Stamatakos, 1997; Wise, 2004) that also attempt to explain other characteristics of the belt, such as the observed lack of tangential shortening or extension that would be expected with bending. In this paper, an alternative approach to assessing regional kinematics is used to examine the proposed models and offer a new scenario for the formation of structures in a salient.

Calcite-twinning analysis provides an independent approach to test the various kinematic hypotheses because it preserves the earliest deformation of rocks along the belt, prior to regional folding. Calcite-twinning analysis shows typical prefolding, layer-parallel deformation patterns that have been recognized in other studies as sensitive indicators of early orogenic evolution (e.g., Engelder, 1979a, 1979b; Ferrill and Groshong, 1993a, 1993b; van der Pluijm et al., 1997; Harris and van der Pluijm, 1998). Deformation experiments on limestones have shown that the bulk orientation of calcite twinning in a sample is dependent on the orientation of the remote stress field (Groshong, 1974; Teufel, 1980; Groshong et al., 1984), which can be extracted from natural samples through data-inversion techniques (Spang, 1972; Evans and Groshong, 1994; Lacombe et al., 1990; Rocher et al., 2004). Twinning of calcite requires a low critical resolved shear stress of ~10 MPa (Jamison and Spang, 1976; Wenk et al., 1987) and is a strain-hardening process, meaning that further twinning is resisted as beds tilt during subsequent deformation. As a consequence, typical deformation conditions recorded by the analysis are those of the early stress field under horizontal compression, producing layer-parallel shortening fabrics (Jamison and Spang, 1976). This paper focuses on results from a detailed study of samples collected along the Pennsylvania salient, which is used to constrain the kinematics and relative timing of deformation events and curvature in the belt.

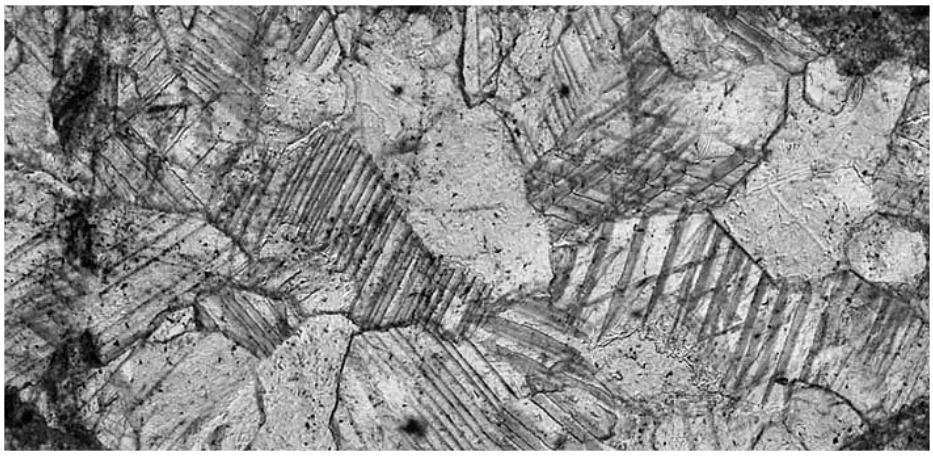

Figure 2. Representative photomicrograph showing twinned calcite grains in plane-polarized light, characterized by single or multiple twin sets and thin twins, which indicate low-temperature conditions. Width of view is ~1 mm.

CALCITE-TWINNING ANALYSIS

The analysis of calcite deformation twins (Fig. 2) as an indicator of paleostress and paleostrain has yielded reliable results both in experimental (Groshong, 1974; Teufel, 1980; Groshong et al., 1984) and in field studies (e.g., Engelder, 1979a, 1979b; Ferrill and Groshong, 1993a, 1993b; van der Pluijm et al., 1997; Kollmeier et al., 2000). Paleostress directions are extracted from a twinned calcite sample by optical determination of the host grain's *c*-axis and the pole to the e-twin plane within the host (Turner, 1953). This information, along with fixed angular relations between the e-twin pole and grain's *c*-axis, yields the most favorable orientation of a compression and extension axis for each twinned grain (Fig. 3). An aggregate of twinned grains is subsequently analyzed for a dominant (or average) compression direction (Spang, 1972). The analysis can involve routines that invert for the stress tensor (Evans and Groshong, 1994; Lacombe and Laurent, 1996; Rocher et al., 2004) or contouring of individual axes in an aggregate, both of which result in paleostress directions that record aspects of the regional stress field. In this study, site directions are analyzed in a geographic and a stratigraphic framework in order to unravel the syn- and post-twinning deformation history of the host rocks. Since deformation of calcite twinning is a strain-hardening process (Teufel, 1980), it typically records early horizontal compression (see also, Chinn and Konig, 1973; Engelder, 1979b; Craddock and van der Pluijm, 1989). Similar to other techniques, such as paleomagnetism, this approach can give insight into tectonic rotations and their relative timing and direction(s) of compression. If multiple, discrete deformation events occurred, they may be recorded as superimposed populations when the deformations are oriented at moderate to high angles to one another (Friedman and Stearns, 1971; Teufel, 1980). In these cases, the events can be extracted by discriminating between twins of a dominant compression direction (expected values, or EVs) and twins of a subordinate compression direction (residual values, or RVs), which are determined on the basis of the feasibility of producing the observed twin with a candidate compression direction. Description of the analysis data-cleaning method can be found in Groshong (1972) and Evans and Groshong (1994), and the procedures used in this study follow our application of calcite-twinning analysis to curvature in the Cantabrian Mountains of northern Spain (Kollmeier et al., 2000).

Oriented samples were collected with a portable, gas-powered diamond coring drill from coarse-grained limestones of the Cambrian-Ordovician Beekmantown Group and Silurian-Devonian Keyser, Helderberg, and Tonoloway Formations. Beside the common occurrence of these units, this stratigraphic sampling strategy was designed to test the Gray and Stamatakos (1997) model, which invokes a hidden detachment between these units. Thin sections from oriented samples were optically analyzed on a universal-stage microscope to determine the crystallographic orientations of twin sets and their host calcite grains (Fig. 3). To ensure optimal measurement of the stress field, we confirmed that samples were not biased by containing crystallographically similarly oriented grains. In addition, we only measured twin sets that were straight and continuous within grains. Using the dynamic analysis of Turner (1953), we determined the compression axes given by the orientation of a grain's *c*-axis and the twin plane, and derived the strain for each sample using the technique of Groshong (1972) and Groshong et al. (1984) for data cleaning. Whereas we did not use strain quantities for our twinning analysis, the orientation of strain axes was used to discriminate between expected values (EVs) and residual values (RVs), as used by Kollmeier et al. (2000), and to identify superimposed deformation phases, if any. Using the resultant spatial stress distribution, we evaluated whether

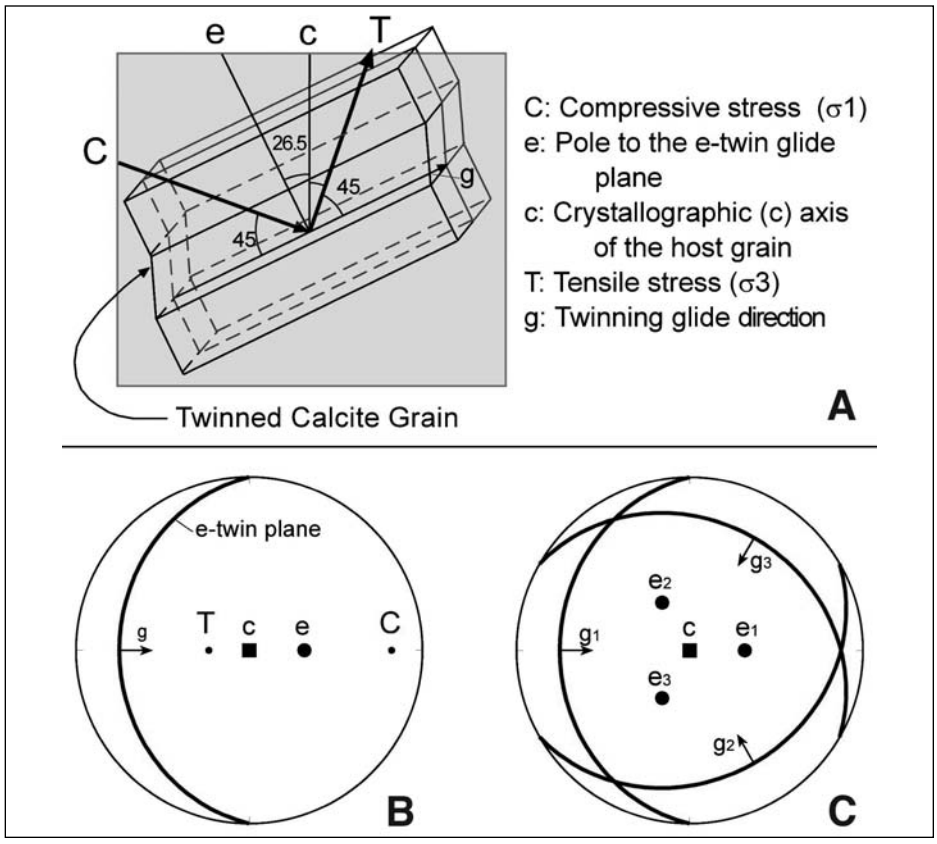

Figure 3. (Top) A calcite grain with a single e-twin and the compressive (C) and tensile (T) stress axes oriented most favorably to produce twinning (oriented 45° to the e-twin plane). The geometric relation of e-twins to *c*-axis is fixed. (Bottom) The same arrangement as shown above but illustrated in a lower-hemisphere equal-area projection that relates the stress orientations to the crystallography. All three possible e-twin planes and their poles are represented (after Kollmeier et al., 2000).

compression was layer-parallel and compared individual site data to geometric models of formation of curved orogenic fronts.

RESULTS

Calcite-twinning analyses of 23 Cambrian-Ordovician and 17 Silurian-Devonian sites along the frontal edge of the salient (Fig. 1; Table 1) were quality-evaluated and reduced to provide reliable paleostress directions for 13 Cambrian-Ordovician and 15 Silurian-Devonian sites. Reliable paleostress directions were also obtained for two sites of Mississippian age in the foreland. Cambrian-Ordovician sites exhibit a dominant population (EVs) of compression directions that are generally orthogonal to regional strike and a residual population (RVs) of subvertical compression directions. Silurian-Devonian sites similarly exhibit a dominant population (EVs) of compression directions orthogonal to regional strike, but also record a small residual population (RVs) of compression directions that are subparallel to strike. We examine in detail only the primary orthogonal signal in both sets of sites, because separation of the residual populations yielded insufficient data for a rigorous analysis of superimposed deformation, but we will comment on the likely significance of other populations.

Within the dominant population, most compression axes lie roughly within or near the bedding plane (Fig. 4), which confirms that twinning records a prefolding, layer-parallel shortening fabric. Where tested, directions from oppositely dipping limbs give coherent directions after bedding correction (i.e., positive fold test). Small deviations from parallelism between compression directions with unfolded bedding are expected due to grain-scale rotations during progressive folding. An amount of deviation from bedding in folded carbonates up to several tens of degrees has been previously documented in calcite-twinning analysis of similar rocks from the Hudson Valley fold-and-thrust belt of the Appalachian orogen by Harris and van der Pluijm (1998) and in paleomagnetic studies in the Pennsylvania salient by Stamatakos and Hirt (1994). Whereas the data from sites along the salient show significant scatter, they follow a systematic change in orientation of paleostress directions that matches the change in regional strike when examined in map view (Fig. 5). We also note that no distinction in the relationship is recognizable between Cambrian-Ordovician and Silurian-Devonian rocks, indicating that these units behaved as a structurally coherent package.

We plotted paleostress directions and paleomagnetic declinations (Table 2) as a function of position along the curvature of the salient in order to quantify the rotations (Fig. 6). Distance along the front is measured from the southwest in a series of linear segments that approximate the along-front distribution of sampling sites. Sites that did not fall along the frontal trend of the salient, such as CO-23 and all paleomagnetic sites, were relocated by projection perpendicular to regional strike. The absence of a difference between Cambrian-Ordovician and Silurian-Devonian samples is clear in this data representation (Fig. 6A). While there is considerable scatter, the rotational pattern is already evident in the raw data. Statistical testing of the data shows that the relationship is significant at the 0.001 level, with a standard error of the slope of 0.049 and a t-value of 4.3. A moving-average analysis of these data using a conservative interval of $n = 3$ (Fig. 7) reduces the inherent scatter of the data, which visually highlights the trend in the raw data set. These moving intervals correspond to 10–40 km segments along the thrust front and yield a data set that we can compare to representative measurements of regional strike taken every 25 km along the thrust front. Note that regional strike representations show proportional but lesser scatter than the raw calcite data (Fig. 6B) and a similar scatter to the moving-averaged calcite data (Fig. 7). There is an excellent match between the slopes of linear best fits to field strike and calcite compression data. By multiplying the best-fit slope of regional strike measurements against the 300 km of sampled frontal distance, we obtain a measure of the full curvature of the salient of ~60 degrees. Best fits to the raw and the moving-averaged data show an equal rotation of paleostress directions of 60–65 degrees along the thrust front, which is statistically identical to the strike rotation. To obtain the orientation in foreland rocks that were not folded, we add analysis of two new sites within the foreland that complement previously published data (Engelder, 1979a, 1979b). These foreland data do not show comparable rotation of compression directions, confirming the systematic regional orientation in foreland

TABLE 1. CALCITE–TWINNING ANALYSIS RESULTS FROM PALEOZOIC ROCKS OF THE PENNSYLVANIA SALIENT, FORELAND SITES, AND SUMMARY OF SITES WITH RESIDUAL POPULATIONS

Site	Lat. (°N)	Long. (°W)	BC distance (km)	Strike sample	Dip	N	Std. err.	% strain	% RV	N RV	Absolute coordinates			Absolute coordinates			Tilt-corrected		Strike	S–S0	D–D0
											e1/elon.	e2/elon.	e3/elon.	σ1	σ2	σ3	σ3	σ3 trd	Regional	Regional	σ3
CO1	40.0023	78.4200	45.3842	22	46 E	25	1.847	5.1	8	2	(67,32)/4.29	(318,28)/1.37	(196,46)–5.66	332,41	75,13	179,46	154,17	154	41	–7	7
CO3	40.3394	78.3940	75.2655	–4	20 E	30	0.857	4.7	0	0	(239,49)/4.33	(36,39)/0.67	(136,12)/–5.00	258,69	51,19	145,9	323,1	143	33	–15	–4
CO4	40.3036	78.2761	79.9156	19	30 E	44	0.258	1.3	14	6	(69,39)/1.25	(256,51)/–0.39	(162,3)/–0.87	335,68	75,4	166,22	160,4	160	39	–9	13
CO7	40.6134	78.1813	113.6662	44	33 E	22	0.803	4.7	0	0	(284,44)/4.56	(37,21)/0.31	(144,39)/–4.87	287,50	44,20	147,32	325,0	145	51	3	–2
CO8	40.6448	78.2331	113.5534	54	68 E	24	0.455	2.1	13	3	(122,20)/1.47	(27,12)/0.88	(268,67)/–2.35	56,10	149,20	303,68	155,42	155	49	1	8
CO9	40.6428	78.0938	129.0225	58	36 E	21	0.333	1.5	5	1	(28,44)/1.51	(288,10)/0.00	(188,44)/–1.51	58,24	303,42	169,39	164,4	164	60	12	17
CO10	40.7985	77.8234	162.1661	26	17 E	20	0.533	2.2	0	0	(49,11)/2.09	(180,74)/0.11	(317,12)/–2.21	59,48	225,41	321,6	323,22	143	64	16	–4
CO11	40.8668	77.8864	159.2826	60	60 W	21	0.503	3.5	0	0	(184,18)/3.18	(84,27)/0.61	(303,57)/–3.78	188,3	97,35	281,54	304,4	124	63	15	–23
CO15	41.0780	77.4870	209.3997	60	60 W	21	0.271	0.9	0	0	(170,48)/0.97	(273,12)/–0.18	(13,40)/–0.78	179,43	277,10	19,45	182,3	182	66	18	35
CO16	40.9428	77.6391	187.3791	54	36 E	26	0.674	5.6	4	1	(279,30)/3.96	(40,42)/2.46	(166,33)/–6.42	263,15	28,64	168,20	347,13	167	59	11	20
CO18	41.0018	77.3795	216.3385	84	18 S	20	0.189	0.5	0	0	(288,17)/2.42	(143,69)/0.91	(22,11)/–3.33	111,42	251,40	0,21	1,39	181	73	25	34
CO23	40.1356	77.7671	113.5534	34	55 E	25	1.127	6.0	0	0	(57,23)/6.49	(231,67)/–1.02	(326,1)/–5.48	212,75	48,14	317,4	327,57	147	46	–2	0
SD1	39.9887	78.6061	29.7415	54	30 E	23	0.383	2.1	0	0	(339,48)/1.65	(235,12)/0.67	(135,39)/–2.33	309,49	207,9	110,39	117,13	117	40	–8	–30
SD4	39.8196	78.6253	15.3556	44	52 E	25	0.587	3.4	0	0	(230,49)/3.27	(2,30)/0.34	(108,25)/–3.60	345,73	222,9	130,14	309.38	129	41	–7	–18
SD5	39.9606	78.5548	30.9155	45	40 E	22	0.657	2.7	0	0	(319,62)/2.87	(224,3)/–0.50	(132,27)/–2.38	267,54	29,21	130,28	310,12	130	40	–8	–17
SD7	40.1069	78.5259	45.6055	28	82 W	22	0.686	2.3	5	1	(210,1)/3.22	(120,29)/0.09	(302,60)/–3.31	195,15	100,21	320,64	128,16	128	19	–29	–19
SD9	40.4208	78.3833	83.6574	98	20 S	19	0.571	2.1	5	1	(208,31)1.89	(61,56)/0.42	(307,16)/–2.31	45,14	162,60	309,26	298,34	118	40	–8	–29
SD10	40.4611	78.4228	85.6198	–40	25 W	21	0.099	0.7	0	0	(60,19)/0.65	(273,68)/0.16	(154,11)/–0.82	46,59	255,29	159,13	163,4	163	35	–13	16
SD11	40.6147	78.3086	106.5545	40	22 W	20	0.092	0.5	100	20	(221,49)/0.33	(19,40)/0.24	(118,11)/–0.56	207,7	100,65	300,23	300,1	120	50	2	–27
SD12	40.1569	78.2999	66.5225	42	68 E	20	0.587	4.0	10	2	(230,10)/2.61	(330,43)/1.94	(130,45)/–4.55	354,41	248,17	140,43	319,24	139	21	–27	–8
SD13	40.5088	78.0737	111.8982	121	10 S	19	0.423	1.7	0	0	(226,24)/1.68	(28,65)/0.04	(134,6)/–1.72	234,44	37,44	136,9	138,6	138	41	–7	–9
SD16	41.0173	76.7819	280.0040	114	17 S	30	0.726	1.6	17	5	(276,9)/1.77	(17,51)/–0.37	(179,38)/–1.39	287,23	41,45	179,38	183,22	183	79	31	36
Foreland Population																					
MC1	40.0548	79.2598	64.9938	55	10 E	25	1.228	4.6	0	0	(48,28)/3.15	(236,61)/2.09	(140,3)/–5.25	34,65	238,24	144,10	324,0	144			
MC2	39.7869	79.1933	49.1000	18	15 E	30	0.812	4.6	3	1	(49,19)/2.97	(272,66)/2.30	(144,15)/–5.26	46,26	265,59	145,17	143,5	143			
"RV" Population																					
CO2	40.1728	78.3818	61.2437	12	48 E	44	0.315	2.5	2	1	(256,49)/2.22	(100,39/0.45	(360,12)/–2.67	199,76	90,5	359,14	14,19	194	30	–18	47
SD2	39.8218	78.7231	7.1506	44	83 W	25	0.612	1.8	4	1	(353,44)/1.92	(252,12)/–0.20	(150,44)/–1.72	336,53	200,28	98,22	17,52	197	35	–17	50
SD3	39.7643	78.7520	0.0000	–20	3 E	22	0.170	0.8	5	1	(206,69)/0.85	(115,0)/–0.05	(25,21)/–0.80	224,63	114,10	19,25	20,23	200	28	–24	53
SD8	40.2678	78.4694	64.1509	64	16 W	29	0.227	1.1	0	0	(214,67)/0.78	(113,6)/0.54	(21,23)/–1.32	183,68	277,2	8,22	6,9	186	19	–29	39
SD14	40.9583	77.7479	177.7241	53	22 N	30	0.591	1.3	17	5	(324,17)/1.51	(88,60)/0.50	(225,23)/–2.01	350,52	151,36	247,9	249,4	249	62	10	102
SD17	41.0300	76.3491	327.1934	104	42 S	31	0.661	2.2	6	2	(144,35)/2.25	(266,38)/–0.15	(27,33)/–2.10	158,49	269,18	13,36	10,78	190	77	25	43

Note: Coordinate data are (direction, plunge)/magnitude; BC is reference distance; S–S0 and D–D0 are difference with reference values.

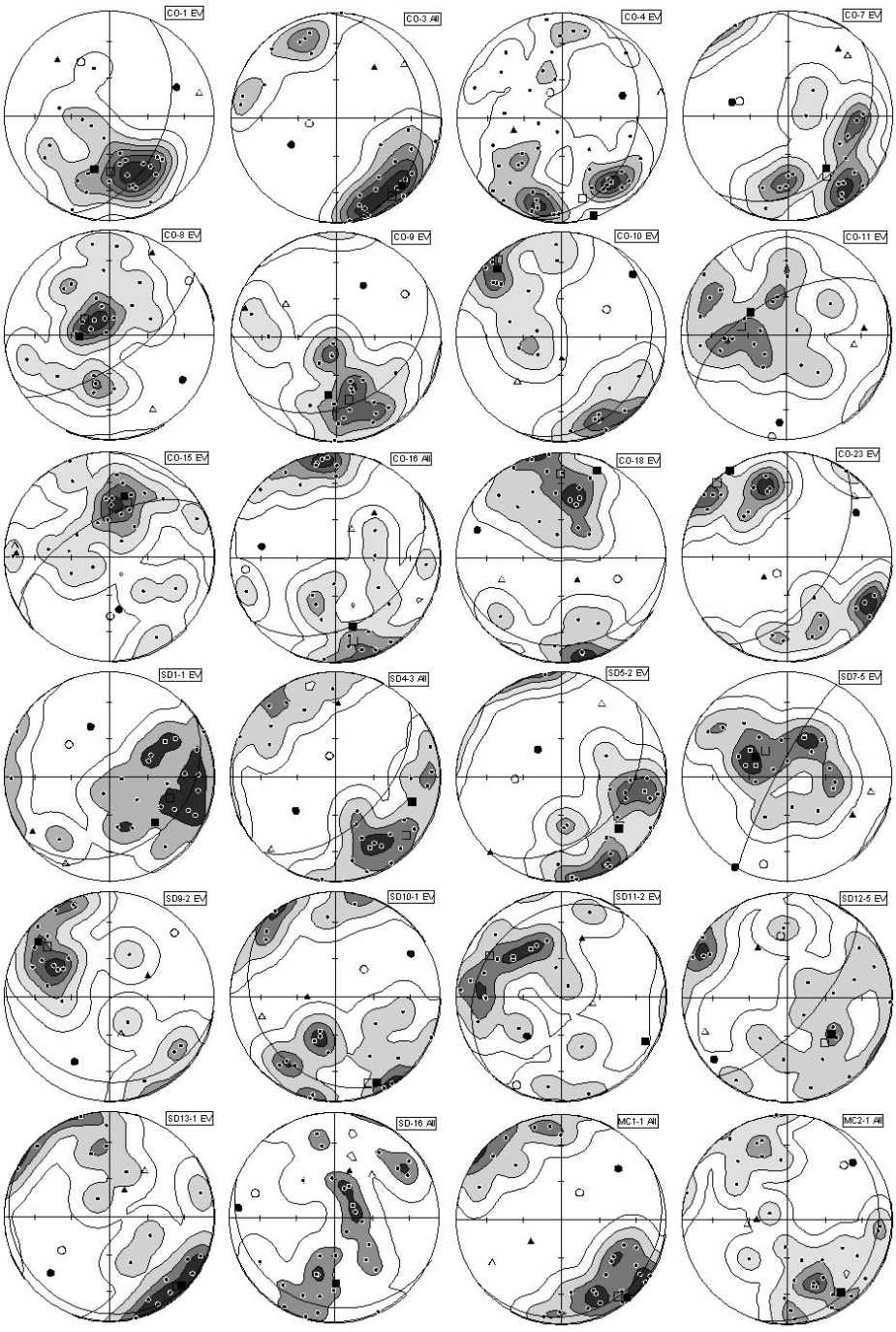

Figure 4. Equal-area lower-hemisphere plots of sample results used in this study. Contoured compressive stress axes (small solid circles) are shown as well as the principal stress and strain axes computed using the Strain99 program after the method of Groshong (1972). All data are represented in present-day field coordinates with bedding included. Other symbols: open square—σ_3, open triangle—σ_2, open circle—σ_1; filled square—e_3, filled triangle—e_2, filled circle—e_1; EV—expected value.

carbonates that has previously been described by Craddock and van der Pluijm (1989) and Craddock et al. (1993).

DISCUSSION

One dominant and two minor populations of compressional directions can be observed from calcite-twinning analysis in the region: a dominant set of directions roughly orthogonal to regional strike that is found in both Cambrian-Ordovician and Silurian-Devonian sites, a small residual set of subvertical directions in Cambrian-Ordovician sites, and a small residual set of strike-parallel directions restricted to Silurian-Devonian sites.

The dominant population of compressional directions varies systematically in orientation that is roughly orthogonal to regional strike. No distinction was found between Lower and Middle/Upper Paleozoic units, and so we reject a previous hypothesis that requires mechanical decoupling between these sequences (e.g., Gray and Stamatakos, 1997). This model also predicted distinct behavior of the magnetization directions, which we tested in a separate paleomagnetic study of Lower Paleozoic units. Results from this study show that magnetization behavior is the same for Lower and Middle/Upper Paleozoic units (Cederquist et al., 2006), which offers additional opposition for their hypothesis. As shown in Figure 7, the indistinguishable trends of compression directions and regional strike, which are distinct from trends in the foreland, show that primary oroclinal bending is responsible for the 60° arcuation of the Pennsylvania salient. The scatter in our data is partly inherent in the structure, as shown by the comparable scatter in regional strike, and is influenced by grain-scale rotations in deformed carbonates that have been documented previously (Harris and van der Pluijm, 1998).

The two minor populations of calcite-twinning data are not sufficiently large to offer conclusive interpretations, but we briefly speculate on their meaning as working hypotheses for our ongoing studies elsewhere along the Appalachian front. The small subvertical population that is evident only in Cambrian-Ordovician rocks is attributed to vertical stresses due to overburden during burial and compaction. The load would otherwise not have been sufficiently large to produce twinning in overlying Silurian-Devonian rocks of the stratigraphic sequence. The minor strike-subparallel population, which is occasionally evident in Silurian-Devonian rocks, may reflect local transpressional stresses. Most importantly, the lack of a widespread residual population indicates the absence of a pervasive secondary compression regime significantly different

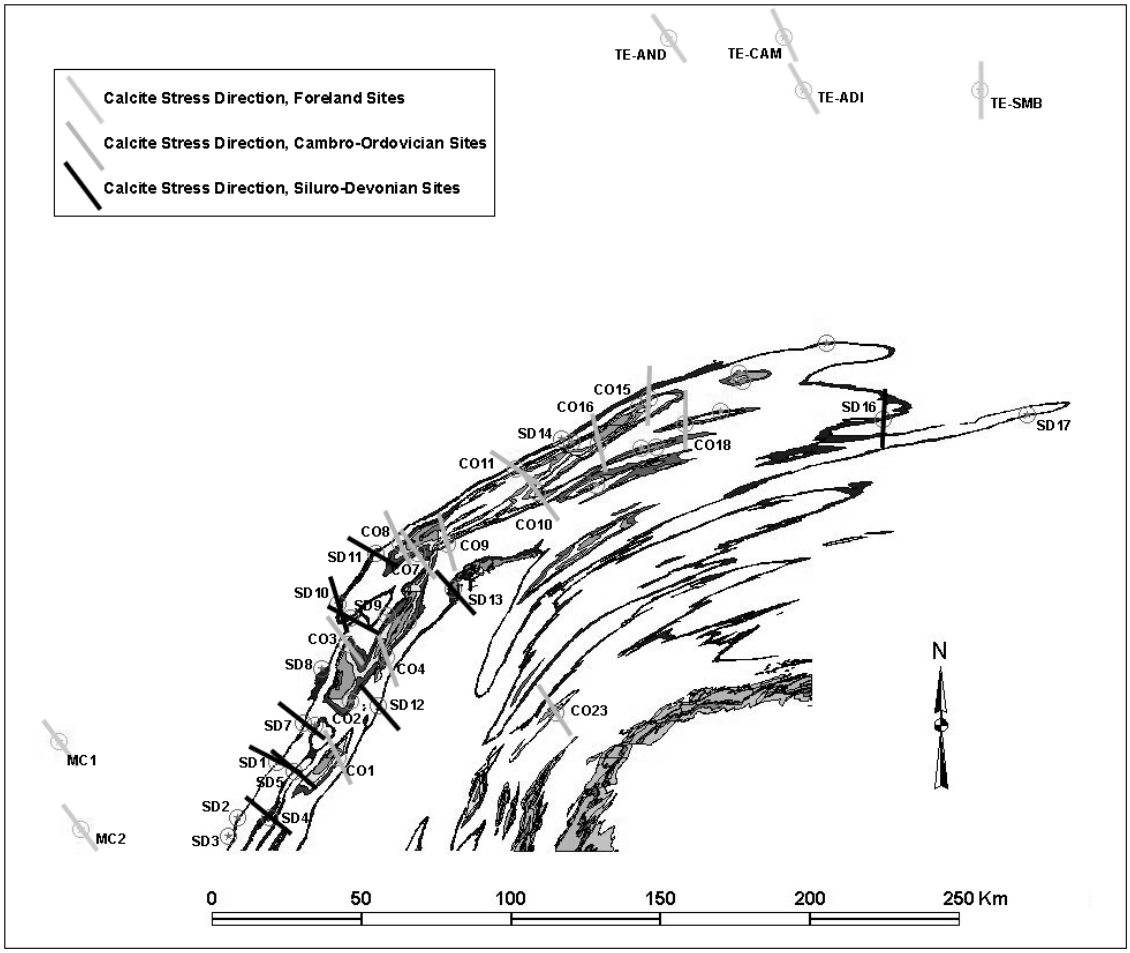

Figure 5. Geographic distribution of tilt-corrected paleostress azimuths (dip-independent) represented by the long direction of bars plotted with respect to geographic north. Bars are shaded according to sample age; dark gray for Cambrian-Ordovician, black for Silurian-Devonian, and light gray for all younger, foreland sites. Sites beginning with the "TE" designation are from Engelder (1979a, 1979b). The Pennsylvania salient is represented by the distribution of carbonate units; light grays represent Cambrian-Ordovician strata, while black represents Silurian-Devonian strata. Site locations are denoted by circled stars; residual value (RV) sites are labeled but do not have plotted directions, while other unusable sites carry no designation.

in orientation from the first. This contrasts, for example, with observations from calcite-twinning analysis in the Cantabrian orocline, where two stress fields could be recognized (Kollmeier et al., 2000).

Timing of Deformation Events

Because compression directions derived from calcite-twinning analysis predate folding and thrusting in the region, they are the earliest indicator of compression and, therefore, early orogenic evolution and tectonic docking. The evidence for the transfer of twinning stresses into weakly deformed continental interior cover rocks (Craddock et al., 1993; van der Pluijm et al., 1997) places additional constraints on the results from this study. The onset of deformation is dated as post–middle Carboniferous in age, because rocks of this age exhibit layer-parallel twinning deformation. Evidence for postrotation, synfolding magnetizations during the Early Permian (Stamatakos et al., 1996; Cederquist et al., 2006) therefore brackets the timing of orogenic bending between Pennsylvanian and Early Permian times (i.e., Alleghanian); i.e., a Pennsylvanian age for oroclinal rotation. Furthermore, since compression directions from calcite-twinning analysis represent the earliest tectonic signal, deformation due to subsequent orogenic processes is recorded by the myriad of other deformation features in the area, such as joint patterns and folding (e.g., Nickelsen, 1979; Gray and Mitra, 1993; Wise, 2004).

Our study recognizes early compression followed by rotation that is not preserved in

TABLE 2. SUMMARY OF PALEOMAGNETIC DATA FROM THE BLOOMBURG FORMATION, AS USED IN FIGURE 6

Site	Lat. (°N)	Long. (°W)	Declination
Cumberland, Maryland	39.7	78.70	147
Mt. Union, Pennsylvania	40.4	77.85	157
Hancock, Maryland	39.7	78.40	165
D–I*	39.7	78.1	165
Round Top, Maryland *	39.6	78.3	166
Danville, Pennsylvania *	40.9	76.7	178
J–L, Q–S*	40.9	76.5	178
O, P*	41.0	76.7	182
Watsontown, Pennsylvania	41.1	76.80	183
Milton, Pennsylvania	41.0	76.85	183
Bloomsburg, Pennsylvania	41.0	76.45	186

Note: Latitude and longitude are taken from Stamatakos and Hirt (1994, their Table 1), if available. Sites designated * have estimates of latitude and longitude based on the other six sites as well as on Stamatakos and Hirt (1994, their Figure 1). Declination is taken from Kent (1988) and Stamatakos and Hirt (1994, their Table 3), converted to represent reversed polarity.

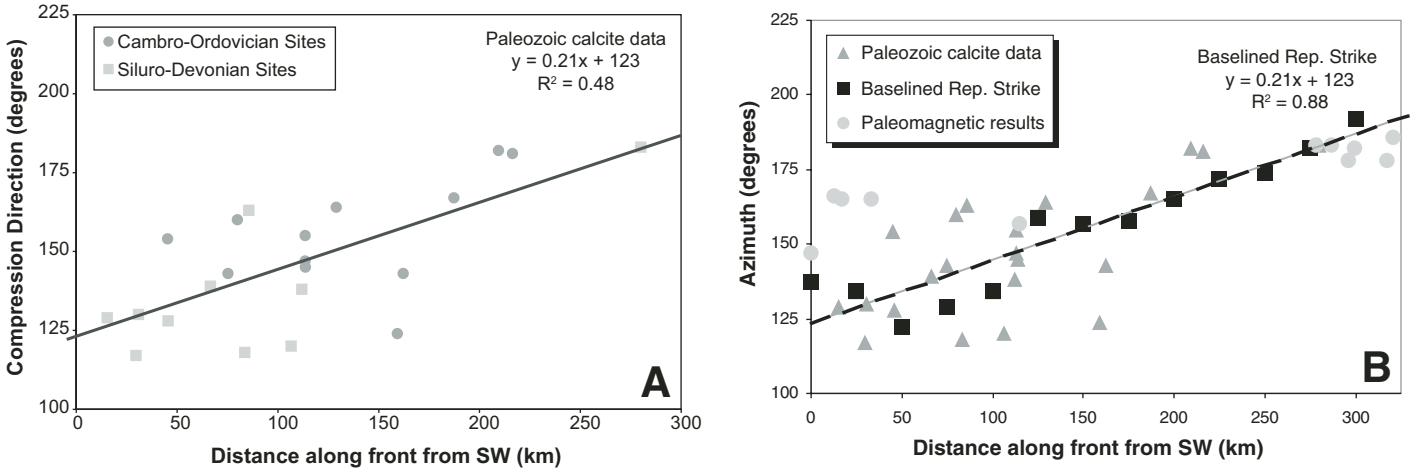

Figure 6. (A) Calcite stress directions as a function of distance along the thrust front. Cambrian-Ordovician sites and Silurian-Devonian sites are distinguished by different symbols and show no difference in trend. The trend line shown is a simple fit to the combined data set. Standard error of the slope is 0.049 and t-value is 4.3, indicating significance of the data set at the 0.001 level (see text for details). (B) As in A but including measurements of representative strike and paleomagnetic declinations (Table 2) for comparison. The trend line through baseline strike is shown and indistinguishable from the trend line of raw data.

other deformation features, with the exception of primary paleomagnetic signals (Kent and Opdyke, 1985; Miller and Kent, 1986a, 1986b; Kent, 1988; Stamatakos and Hirt, 1994). These paleomagnetic data (Table 2) display a similar trend of rotation to the calcite-twinning data (Fig. 6B), but the total magnitude of rotation appears to be less than that documented in our study, which remains to be explained. Regardless, the paleomagnetic data document a similar systematic change in direction commensurate with a change in strike that falls within the range from calcite data.

Regional Kinematic Scenario

We attempt to integrate all available data into a spatio-temporal evolutionary model for this curved portion of the Appalachian belt (Fig. 8), which will also serve as a testable hypothesis for work elsewhere along the orogenic front and perhaps a tectonic signature for other curved orogens (e.g., the Rocky Mountains). Upon collision at the Laurentian margin, calcite in units as young as mid-Carboniferous became twinned in a dominantly uniform stress field that is today preserved in foreland carbonates. Strain-hardening locked the initial stress directions as passive markers in carbonate strata. Next, vertical-axis rotations up to ~60° reoriented these paleostress directions in calcite, providing the bulk of angular rotation that is evident in the present day. This rotation produced a crustal heterogeneity that affected subsequent deformation in the area. When folding occurred during the Early Permian, regional folds with curved axial surfaces formed in their present configuration, following the structural anisotropy imposed by the earlier rotation. In this scenario, the early deformation, characterized by thrusting and rotation, was temporally separate from later folding of the cover sequence.

The formation of folds with curved trends explains the absence of tangential compression or extension along the belt, as described by Wise (2004). The scenario also explains the absence of evidence for rotation in remagnetized rocks (e.g., Gray and Stamatakos, 1997; Cederquist et al., 2006). During folding in the Early Permian, secondary magnetization progressed from the hinterland to the foreland and produced a postfolding magnetization in hinterland folds, a prefolding magnetization in the rotated foreland, and a synfolding pattern in between (Gray and Stamatakos, 1997; Cederquist et al., 2006).

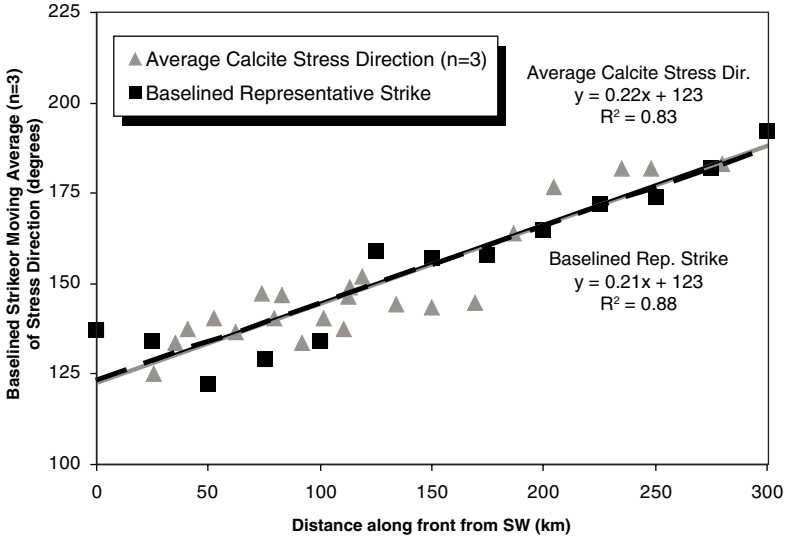

Figure 7. Moving window analysis of combined calcite paleostress directions, using averages of $n = 3$ (triangles) as a function of distance along thrust front. Representative strike along the thrust front is plotted schematically with a *y*-axis shift of 99° for comparison (squares). Best-fit lines for both data are shown and fully overlap. The arbitrary value of 99° is used solely because it causes the *y*-intercepts to coincide and allows for a better visual comparison of the slope.

Since this fold-related pattern and remagnetization postdate rotation in our scenario, past interpretations that have required more complicated deformation histories to explain the observations are significantly simplified.

Finally, the orientation of calcite-twinning patterns in foreland sites from this study and others (Engelder, 1979a, 1979b; Craddock et al., 1993) can be interpreted to indicate oblique convergence at the Laurentian margin, resulting in left-lateral transpression in the southern segment of the Appalachian salient and dextral transpression in the northern segment of the salient in Pennsylvanian times. Comparison of compression directions from within the orocline to those in the foreland yields a close match with the southern limb of the salient, which we interpret as pinning of the southern region while the northern segment of the salient accommodated most of the rotation. Rotation of the northern segment is also in agreement with paleomagnetically determined rotations in the area (Van der Voo, 1993, p. 79).

Whereas our kinematic data cannot preclude a role for lateral variations in wedge thickness in the rotations (Macedo and Marshak, 1999), we mostly attribute the pattern of rotation to the presence of Precambrian rocks, the Adirondacks and Reading Prong (see Thomas, 2006, for a recent description of the plate-margin geometry), which acted as a barrier to oblique convergence and created the present-day Pennsylvania salient by rotation of its northern limb.

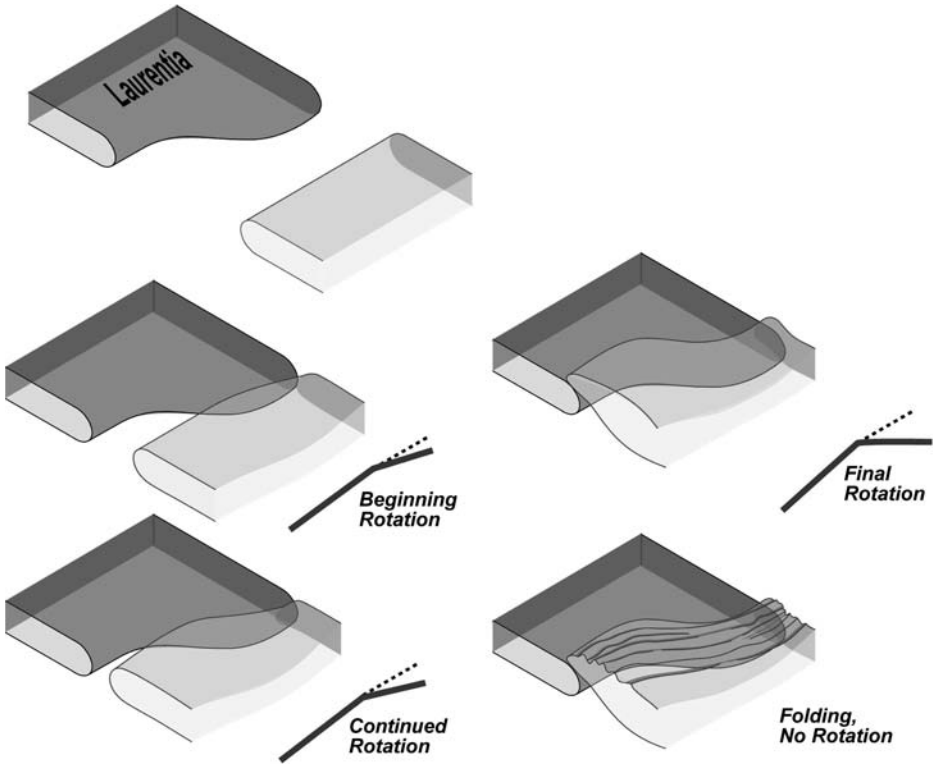

Figure 8. Spatio-temporal scenario for the evolution of the Pennsylvania salient with a Laurentian basement heterogeneity, based on calcite twinning and (re)magnetization data. In Pennsylvanian times, oblique collision resulted in penetrative calcite twinning, with progressive rotation of imparted stress directions at Proterozoic promontory. Rotation is (partly) tracked by primary magnetizations. In Early Permian times, termination of rotation (wedge locking) occurred, resulting in the development of cover folds that track the preexisting curvature. The folding stage was accompanied by remagnetization.

CONCLUSIONS

Calcite-twinning analysis provides an independent data set that can be used to examine the origin of curvature in the Pennsylvania salient. We find rotation of paleostress directions up to 60° within the salient, compared to a dominantly uniform stress field that is preserved in the neighboring foreland and other mid-continent sites. Penetrative calcite twinning in the orogen and foreland occurred prior to Early Permian folding. Rotation of the belt was associated with Pennsylvanian thrusting, but this event was temporally separated from younger folding. This temporal sequence may reflect regional folding after the thrust wedge was locked in the Early Permian. Folding is associated with widespread remagnetization, while fold axial traces track the curved crustal grain (i.e., a mechanical anisotropy) from earlier thrusting. This scenario may also be applicable to curved orogenic fronts elsewhere, such as the Wyoming salient in the U.S. Rocky Mountains (e.g., Eldredge et al., 1985; Craddock et al., 1988; Paulsen and Marshak, 1997), where it is important to characterize the presence of preexisting basement heterogeneities.

Thus, strictly speaking, rotation in the Pennsylvania salient is of secondary origin, but it preceded regional folds with curved trajectories that were otherwise unrotated. Fold curvature, therefore, is primary in origin. Because convergence directions in the foreland best match those of the southern limb of the salient, we suggest that most of the rotation was accommodated in the northern limb, as has also been suggested by paleomagnetic studies. We propose that a Precambrian basement block of the Adirondacks and Reading Prong acted as a buttress that caused early rotation.

ACKNOWLEDGMENTS

This project was supported by a grant from the American Chemical Society Petroleum Research Fund (#37505-AC2), a Geological Society of America Student Research Grant, and the Scott M. Turner Fund of the University of Michigan. We thank Mike Allis for invaluable assistance in the field and the journal reviewers and associate editor for critical comments that significantly sharpened the presentation of our results.

REFERENCES CITED

Carey, S.W., 1955, The orocline concept in geotectonics: Proceedings of the Royal Society of Tasmania, v. 89, p. 255–289.

Cederquist, D.P., Van der Voo, R., and van der Pluijm, B.A., 2006, Syn-folding remagnetization of Cambro-Ordovician carbonates from the Pennsylvania salient postdates oroclinal rotation: Tectonophysics, v. 422, p. 41–54, doi: 10.1016/j.tecto.2006.05.005.

Chinn, A.A., and Konig, R.H., 1973, Stress inferred from calcite twin lamellae in relation to regional structure of northwest Arkansas: Geological Society of America Bulletin, v. 84, p. 3731–3736, doi: 10.1130/0016-7606(1973)84<3731:SIFCTL>2.0.CO;2.

Craddock, J.P., and van der Pluijm, B.A., 1989, Late Paleozoic deformation of the cratonic carbonate cover of eastern North America: Geology, v. 17, p. 416–419, doi: 10.1130/0091-7613(1989)017<0416:LPDOTC>2.3.CO;2.

Craddock, J.P., Kopania, A.A., and Wiltschko, D.V., 1988, Interaction between the northern Idaho-Wyoming thrust belt and bounding basement blocks, central western Wyoming, *in* Schmidt, C.J., and Perry, W.J., eds., Interaction of the Rocky Mountain Foreland and the Cordilleran Thrust Belt: Geological Society of America Memoir 171, p. 333–351.

Craddock, J.P., Jackson, M., van der Pluijm, B.A., and Versical, R.T., 1993, Regional shortening fabrics in eastern North America: Far-field stress transmission from the Appalachian-Ouachita orogenic belt: Tectonics, v. 12, p. 257–264.

Eldredge, S., Bachtadse, V., and Van der Voo, R., 1985, Paleomagnetism and the orocline hypothesis: Tectonophysics, v. 119, p. 153–179, doi: 10.1016/0040-1951(85)90037-X.

Engelder, T., 1979a, Mechanisms for strain within the Upper Devonian clastic sequence of the Appalachian Plateau, western New York: American Journal of Science, v. 279, p. 527–542.

Engelder, T., 1979b, The nature of deformation within the outer limits of the central Appalachian foreland fold and thrust belt in New York State: Tectonophysics, v. 55, p. 289–310, doi: 10.1016/0040-1951(79)90181-1.

Evans, M.A., and Groshong, R.H., 1994, A computer program for the calcite strain-gauge technique: Journal of Structural Geology, v. 16, p. 277–282, doi: 10.1016/0191-8141(94)90110-4.

Ferrill, D.A., and Groshong, R.H., 1993a, Kinematic model for the curvature of the northern Subalpine Chain, France: Journal of Structural Geology, v. 15, p. 523–541, doi: 10.1016/0191-8141(93)90146-2.

Ferrill, D.A., and Groshong, R.H., 1993b, Deformation conditions in the northern Subalpine Chain, France, estimated from deformation modes in coarse-grained limestone: Journal of Structural Geology, v. 15, p. 995–1006, doi: 10.1016/0191-8141(93)90172-7.

Friedman, M., and Stearns, D.W., 1971, Relations between stresses inferred from calcite twin lamellae and macrofractures, Teton anticline, Montana: Geological Society of America Bulletin, v. 82, p. 3151–3162.

Geiser, P., and Engelder, T., 1983, The distribution of layer-parallel shortening fabrics in the Appalachian foreland of New York and Pennsylvania: Evidence for two non-coaxial phases of the Alleghenian orogeny, *in* Hatcher, R.D., Jr., Williams, H., and Zietz, I., eds., Contributions to the tectonics and geophysics of mountain chains: Geological Society of America Memoir 158, p. 161–175.

Gray, M.B., and Mitra, G., 1993, Migration of deformation fronts during progressive deformation: Evidence from detailed structural studies in the Pennsylvania Anthracite Region, U.S.A.: Journal of Structural Geology, v. 15, p. 435–449, doi: 10.1016/0191-8141(93)90139-2.

Gray, M.B., and Stamatakos, J., 1997, New model for evolution of fold and thrust belt curvature based on integrated structural and paleomagnetic results from the Pennsylvania salient: Geology, v. 25, p. 1067–1070, doi: 10.1130/0091-7613(1997)025<1067:NMFEOF>2.3.CO;2.

Groshong, R.H., 1972, Strain calculated from twinning in calcite: Geological Society of America Bulletin, v. 83, p. 2025–2038.

Groshong, R.H., 1974, Experimental test of least-squares strain gage calculation using twinned calcite: Geological Society of America Bulletin, v. 85, p. 1855–1864, doi: 10.1130/0016-7606(1974)85<1855:ETOLSG>2.0.CO;2.

Groshong, R.H., Teufel, L.W., and Gasteiger, C., 1984, Precision and accuracy of the calcite strain-gage technique: Geological Society of America Bulletin, v. 95, p. 357–363, doi: 10.1130/0016-7606(1984)95<357:PAAOTC>2.0.CO;2.

Harris, J.H., and van der Pluijm, B.A., 1998, Relative timing of calcite twinning strain and fold-thrust belt development; Hudson Valley fold-thrust belt, New York, U.S.A.: Journal of Structural Geology, v. 20, p. 21–31, doi: 10.1016/S0191-8141(97)00093-X.

Hindle, D., and Burkhard, M., 1999, Strain, displacement and rotation associated with the formation of curvature in fold belts; the example of the Jura arc: Journal of Structural Geology, v. 21, p. 1089–1101, doi: 10.1016/S0191-8141(99)00021-8.

Hobbs, W.H., 1914, Mechanics of formation of arcuate mountains: The Journal of Geology, v. 102, p. 71–90.

Jamison, W.R., and Spang, J.H., 1976, Use of calcite twin lamellae to infer differential stress: Geological Society of America Bulletin, v. 87, p. 868–872, doi: 10.1130/0016-7606(1976)87<868:UOCTLT>2.0.CO;2.

Kent, D.V., 1988, Further paleomagnetic evidence for oroclinal rotation in the central folded Appalachians from the Bloomsburg and the Mauch Chunk Formations: Tectonics, v. 7, p. 749–759.

Kent, D.V., and Opdyke, N.D., 1985, Multicomponent magnetization from the Mississippian Mauch Chunk Formation of the central Appalachians and their tectonic implications: Journal of Geophysical Research, v. 90, p. 5371–5383.

Kollmeier, J.M., van der Pluijm, B.A., and Van der Voo, R., 2000, Analysis of Variscan dynamics; early bending of the Cantabria-Asturias Arc, northern Spain: Earth and Planetary Science Letters, v. 181, p. 203–216, doi: 10.1016/S0012-821X(00)00203-X.

Lacombe, O., and Laurent, P., 1996, Determination of deviatoric stress tensors based on inversion of calcite twin data from experimentally deformed monophase samples: Preliminary results: Tectonophysics, v. 255, p. 189–202, doi: 10.1016/0040-1951(95)00136-0.

Lacombe, O., Angelier, J., Bergerat, F., Laurent, P., and Tourneret, C., 1990, Joint analysis of calcite twins and fault slips as a key for deciphering polyphase tectonics: Burgundy as a case study: Tectonophysics, v. 182, p. 279–300, doi: 10.1016/0040-1951(90)90168-8.

Macedo, J., and Marshak, S., 1999, Controls on the geometry of fold-thrust belt salients: Geological Society of America Bulletin, v. 111, p. 1808–1822, doi: 10.1130/0016-7606(1999)111<1808:COTGOF>2.3.CO;2.

Marshak, S., 1988, Kinematics of orocline and arc formation in thin-skinned orogens: Tectonics, v. 7, p. 73–86.

Marshak, S., 2004, Salients, recesses, arcs, oroclines, and syntaxes—A review of ideas concerning the formation of map-view curves in fold-thrust belts, *in* McClay, K.R., ed., Thrust Tectonics and Hydrocarbon Systems: American Association of Petroleum Geologists Memoir 82, p. 131–156.

Miller, J.D., and Kent, D.V., 1986a, Paleomagnetism of the Upper Devonian Catskill Formation from the southern limb of the Pennsylvania salient: Possible evidence of oroclinal rotation: Geophysical Research Letters, v. 13, p. 1173–1176.

Miller, J.D., and Kent, D.V., 1986b, Synfolding and prefolding magnetizations in the Upper Devonian Catskill Formation of eastern Pennsylvania: Implications for the tectonic history of Acadia: Journal of Geophysical Research, v. 91, p. 12,791–12,803.

Nickelsen, R.P., 1979, Sequence of structural stages of the Alleghany orogeny, Bear Valley strip mine, Shamokin, PA: American Journal of Science, v. 279, p. 225–271.

Paulsen, T., and Marshak, S., 1997, Structure of the Mount Raymond transverse zone at the southern end of the Wyoming salient, Sevier fold-thrust belt, Utah: Tectonophysics, v. 280, no. 3–4, p. 199–211, doi: 10.1016/S0040-1951(97)00205-9.

Rocher, M., Cushing, M, Lemeille, F., Lozac'h, Y., and Angelier, J., 2004, Intraplate paleostresses reconstructed with calcite twinning and faulting: Improved method and application to the eastern Paris Basin (Lorraine, France): Tectonophysics, v. 387, p. 1–21, doi: 10.1016/j.tecto.2004.03.002.

Spang, J.H., 1972, Numerical method for dynamic analysis of calcite twin lamellae: Geological Society of America Bulletin, v. 83, p. 467–472.

Spraggins, S.A., and Dunne, W.M., 2002, Deformation history of the Roanoke recess, Appalachians, USA: Journal of Structural Geology, v. 24, p. 411–433, doi: 10.1016/S0191-8141(01)00077-3.

Stamatakos, J., and Hirt, A.M., 1994, Paleomagnetic considerations of the development of the Pennsylvania salient in the central Appalachians: Tectonophysics, v. 231, p. 237–255, doi: 10.1016/0040-1951(94)90037-X.

Stamatakos, J., Hirt, A.M., and Lowrie, W., 1996, The age and timing of folding in the central Appalachians from paleomagnetic results: Geological Society of America Bulletin, v. 108, p. 815–829, doi: 10.1130/0016-7606(1996)108<0815:TAATOF>2.3.CO;2.

Sussman, A.J., Butler, R.F., Dinares-Turell, J., and Verges, J., 2004, Vertical-axis rotation of a foreland fold and implications for orogenic curvature: An example from the Southern Pyrenees, Spain: Earth and Planetary Science Letters, v. 218, p. 435–449, doi: 10.1016/S0012-821X(03)00644-7.

Teufel, L.W., 1980, Strain analysis of experimental superposed deformation using calcite twin lamellae: Tectonophysics, v. 65, p. 291–309, doi: 10.1016/0040-1951(80)90079-7.

Thomas, W.A., 2006, Tectonic inheritance at a continental margin: GSA Today, v. 16, p. 4–11, doi: 10.1130/1052-5173(2006)016[4:TIAACM]2.0.CO;2.

Turner, F.J., 1953, Nature and dynamic interpretation of deformation lamellae in calcite of three marbles: American Journal of Science, v. 251, p. 276–298.

van der Pluijm, B.A., Craddock, J.P., Graham, B.R., and Harris, J.H., 1997, Paleostress in cratonic North America: Implications for deformation of continental interiors: Science, v. 277, p. 794–796, doi: 10.1126/science.277.5327.794.

Van der Voo, R., 1993, Paleomagnetism of the Atlantic, Tethys, and Iapetus Oceans: Cambridge, UK, Cambridge University Press, 424 p.

Weil, A.B., and Sussman, A.J., 2004, Classifying curved orogens based on timing relationships between structural development and vertical-axis rotations, *in* Sussman, A.J., and Weil, A.B., eds., Orogenic Curvature: Integrating Paleomagnetic and Structural Analysis: Geological Society of America Special Paper 383, p. 1–15.

Weil, A.B., Van der Voo, R., van der Pluijm, B.A., and Pares, J., 2000, The formation of an orocline by multiphase deformation; a paleomagnetic investigation of the Cantabria Asturias Arc (northern Spain): Journal of Structural Geology, v. 22, p. 735–756, doi: 10.1016/S0191-8141(99)00188-1.

Wenk, H.R., Takeshita, T., Bechler, E., Erskine, B.G., and Matthies, S., 1987, Pure shear and simple shear calcite textures. Comparison of experimental, theoretical and natural data: Journal of Structural Geology, v. 9, p. 731–745, doi: 10.1016/0191-8141(87)90156-8.

Wise, D.U., 2004, Pennsylvania salient of the Appalachians: A two-azimuth transport model based on new compilations of Piedmont data: Geology, v. 32, no. 9, p. 777–780, doi: 10.1130/G20547.1.

Younes, A., and Engelder, T., 1999, Fringe cracks: A key data set for the interpretation of progressive Alleghenian deformation of the Appalachian Plateau: Geological Society of America Bulletin, v. 111, p. 219–239, doi: 10.1130/0016-7606(1999)111<0219:FCKSFT>2.3.CO;2.

Zhao, M., and Jacobi, R.D., 1997, Formation of regional cross-fold joints in the northern Appalachian Plateau: Journal of Structural Geology, v. 19, p. 817–834, doi: 10.1016/S0191-8141(97)00009-6.

Manuscript Received 31 March 2006
Revised Manuscript Received 9 August 2006
Manuscript Accepted 3 September 2006

Printed in the USA